
























RESEARCH PAPER

SPECIAL SERIES ON HOST-MICROBIOME-HOMEOSTASIS

Metformin modulates microbiota and improves blood pressure and cardiac remodeling in a rat model of hypertension

Moritz I. Wimmer^{1,2,3,4}  | Hendrik Bartolomaeus^{1,2,3,4}  | Harithaa Anandakumar^{1,2,3,4}  |
 Chia-Yu Chen^{2,3,4,5}  | Valentin Vecera^{1,2,3,4}  | Sarah Kedziora^{2,3,4,5}  |
 Sakshi Kamboj⁶  | Fabian Schumacher⁷  | Sidney Pals² | Ariana Rauch^{1,2,3,4}  |
 Jutta Meisel^{2,3,5} | Olena Potapenko^{1,2,3}  | Alex Yarritu^{1,2,3,4}  |
 Theda U. P. Bartolomaeus^{2,3,4,5}  | Mariam Samaan^{2,3,5}  | Arne Thiele^{1,2,3,4}  |
 Lucas Stürzbecher^{2,8,9} | Sabrina Y. Geisberger^{3,4}  | Burkhard Kleuser⁷  |
 Peter J. Oefner⁶  | Nadine Haase^{2,3,4,5}  | Ulrike Löber^{2,3,4,5}  |
 Wolfram Gronwald⁶  | Sofia K. Forslund-Startceva^{2,3,4,5,10}  |
 Dominik N. Müller^{2,3,4,5}  | Nicola Wilck^{1,2,3,4} 

¹Department of Nephrology and Medical Intensive Care Medicine, Charité—Universitätsmedizin Berlin, Freie Universität Berlin and Humboldt-Universität zu Berlin, Berlin, Germany

²Experimental and Clinical Research Center (ECRC), Charité—Universitätsmedizin Berlin, Max Delbrück Center for Molecular Medicine, Berlin, Germany

³Max-Delbrück-Center for Molecular Medicine in the Helmholtz Association, Berlin, Germany

⁴DZHK (German Centre for Cardiovascular Research), Berlin, Germany

⁵Charité—Universitätsmedizin Berlin, Freie Universität Berlin and Humboldt-Universität zu Berlin, Berlin, Germany

⁶Institute of Functional Genomics, University of Regensburg, Regensburg, Germany

⁷Institute of Pharmacy, Freie Universität Berlin, Berlin, Germany

⁸Department of Ophthalmology, Charité—Universitätsmedizin Berlin, Freie Universität Berlin and Humboldt-Universität zu Berlin, Berlin, Germany

⁹Eye Center, Medical Center, Faculty of Medicine, University of Freiburg, Freiburg, Germany

¹⁰Structural and Computational Biology Unit, European Molecular Biology Laboratory (EMBL), Heidelberg, Germany

Correspondence

Nicola Wilck, Charité—
 Universitätsmedizin Berlin,
 Lindenberger Weg 80, 13125 Berlin,
 Germany.
 Email: nicola.wilck@charite.de

Present address

Hendrik Bartolomaeus, Institute of
 Experimental Biomedicine, University
 Hospital Würzburg, Würzburg,
 Germany

Abstract

Aims: Metformin has been attributed to cardiovascular protection even in the absence of diabetes. Recent observations suggest that metformin influences the gut microbiome. We aimed to investigate the influence of metformin on the gut microbiota and hypertensive target organ damage in hypertensive rats.

Methods: Male double transgenic rats overexpressing the human renin and angiotensinogen genes (dTGR), a model of angiotensin II-dependent hypertension, were treated with metformin (300 mg/kg/day) or vehicle from 4 to 7 weeks of age.

Moritz I. Wimmer and Hendrik Bartolomaeus contributed equally to this study.

This is an open access article under the terms of the [Creative Commons Attribution](https://creativecommons.org/licenses/by/4.0/) License, which permits use, distribution and reproduction in any medium, provided the original work is properly cited.

© 2024 The Author(s). *Acta Physiologica* published by John Wiley & Sons Ltd on behalf of Scandinavian Physiological Society.

Funding information

Deutsche Forschungsgemeinschaft;
Deutsches Zentrum für Herz-
Kreislaufforschung

We assessed gut microbiome composition and function using shotgun metagenomic sequencing and measured blood pressure via radiotelemetry. Cardiac and renal organ damage and inflammation were evaluated by echocardiography, histology, and flow cytometry.

Results: Metformin treatment increased the production of short-chain fatty acids (SCFA) acetate and propionate in feces without altering microbial composition and diversity. It significantly reduced systolic and diastolic blood pressure and improved cardiac function, as measured by end-diastolic volume, E/A, and stroke volume despite increased cardiac hypertrophy. Metformin reduced cardiac inflammation by lowering macrophage infiltration and shifting macrophage subpopulations towards a less inflammatory phenotype. The observed improvements in blood pressure, cardiac function, and inflammation correlated with fecal SCFA levels in dTGR. In vitro, acetate and propionate altered M1-like gene expression in macrophages, reinforcing anti-inflammatory effects. Metformin did not affect hypertensive renal damage or microvascular structure.

Conclusion: Metformin modulated the gut microbiome, increased SCFA production, and ameliorated blood pressure and cardiac remodeling in dTGR. Our findings confirm the protective effects of metformin in the absence of diabetes, highlighting SCFA as a potential mediators.

KEYWORDS

cardiac remodeling, hypertension, inflammation, metformin, microbiome, short-chain fatty acids

1 | INTRODUCTION

Metformin, a long-established first-line medication for type 2 diabetes,¹ has attracted the attention of researchers for its potential benefits beyond diabetes. The observed cardiovascular benefits in diabetic patients^{2,3} have prompted investigations into its cardioprotective role in non-diabetic conditions both preclinically^{4,5} and clinically.^{6,7} However, despite the wide range of effects under diabetic and non-diabetic states, the precise mechanisms underpinning metformin's actions remain insufficiently understood.^{8–10} Interestingly, intravenous administration of metformin fails to elicit changes in blood glucose levels or glucose metabolism, suggesting the need for gastrointestinal passage and a potential role for the intestinal microbiome in mediating the therapeutic effects of metformin.^{11,12} In line, fecal transplants from metformin-treated donors to germ-free mice improved the recipient's glucose tolerance,¹³ and antibiotic depletion of the gut microbiota nullified the metformin-induced antihyperglycemic effects in mouse models,⁴ underscoring the modulatory role of the gut microbiota in mediating metformin's actions.

In humans, metformin treatment has been shown to influence gut microbiome composition and function in different ways.^{13–16} While the production of protective

short-chain fatty acids (SCFA) was observed on one hand, a potential increase in lipopolysaccharides (LPS) was observed on the other.¹⁴ SCFA are of major interest in the prevention of cardiovascular disease and have been demonstrated to modulate blood pressure as well as confer organ protection from hypertensive damage through their immunomodulatory properties.^{17–22}

Accumulating evidence suggests that either direct administration of SCFA or dietary fiber interventions that promote the generation of SCFA by the gut microbiome can exert antihypertensive effects and improve blood pressure management in hypertensive patients.^{7,23} The interaction of dietary fiber, SCFA, and blood pressure has recently been reviewed in depth by Marques and colleagues.²⁴ It has long been recognized that inflammation plays a critical role in hypertension and especially hypertensive target organ damage.²⁵ While available pharmaceutical approaches address hemodynamic load, no current therapeutic approach deals with the inflammatory phenotype. The double transgenic rat (dTGR) model, overexpressing human renin and angiotensinogen genes on a Sprague–Dawley (SD) background,²⁶ is a well-established model of angiotensin II-dependent hypertension and exhibits a remarkable inflammatory response^{27–29} to hypertension and consequently succumb

to cardio-renal damage with a limited lifespan.^{30,31} The elevated angiotensin II levels in dTGR drive the development of hypertension and subsequent cardio-renal injury, making it an ideal preclinical model for evaluating the effects of novel pharmaceutical approaches on hypertension.^{27,31–33}

The present study sought to elucidate the impact of metformin on cardio-renal damage, inflammation, and the gut microbiome composition, offering insights into the putative mechanisms that could account for metformin's therapeutic potential in cardiovascular disease management, even in non-diabetic conditions.

2 | RESULTS

2.1 | Metformin treatment of non-diabetic hypertensive rats

To investigate the impact of metformin on hypertensive damage and the gut microbiome in the absence of diabetes, we administered metformin to male dTGR at a dose of 300 mg/kg body weight per day through their drinking water.³⁴ The control group received equimolar magnesium chloride (vehicle) via the drinking water. Untreated, age-matched male SD rats were used as a non-hypertensive reference for parts of the comparisons. The dTGR model is characterized by elevated blood pressure already at weaning.^{26,30,31} Treatment was initiated after weaning at 4 weeks of age until 7 weeks of age. Untreated dTGR experience spontaneous mortality starting from 7 weeks of age.^{26,30,31} Notably, no mortality was observed in any group, as the animals were sacrificed before reaching 7 weeks of age according to the 3R principle. Metformin treatment was well tolerated, as the body weight remained stable in metformin and vehicle-treated dTGR (Figure S1A,B), and plasma metformin concentrations were within the normal therapeutic range observed in humans³⁵ (Figure S1C). Albeit plasma glucose and lactate levels were slightly elevated in metformin-treated dTGR, no signs of lactate acidosis were detected (Figure S1D,E).

2.2 | Metformin modulates gut microbial function

To assess the influence of metformin on gut microbiome structure and function, we collected fecal samples weekly from before the treatment (week 4) until the end of the study in week 7. Shotgun metagenomic sequencing of fecal samples revealed no changes in alpha diversity upon metformin treatment, as assessed by the Shannon diversity

index and Pielou evenness index (Figure 1A, Figure S2A). Beta diversity analysis by Bray–Curtis dissimilarity showed no clustering by treatment or timepoint (Figure 1B). Similarly, no significant shifts were observed in the phylum level composition of the gut microbiome (Figure 1C). Consistent with previous data from large human cohorts,^{14–16} metformin led to a significant increase in the production potential of the SCFA propionate and acetate 1 week after treatment initiation (Figure 1D,F) as assessed by shotgun sequencing. This finding was corroborated by the measurement of increased fecal levels of propionate and acetate in metformin-treated dTGR compared to vehicle at the endpoint (Figure 1E,G). While SD rats generally had higher acetate and propionate levels, metformin significantly increased the levels in dTGR towards the SD reference. In contrast, butyrate and 3-hydroxyisobutyrate levels remained unchanged (Figure S2B,C). The increase in acetate and propionate levels was consistent across different cohorts (Figure S2D,E). However, the elevated gut microbial SCFA production potential assessed by shotgun metagenomics was not sustained at later time points (Figure S2F). Furthermore, we evaluated the LPS production potential by shotgun sequencing and measured LPS serum levels, as previous reports^{14–16} indicated increased microbial LPS production as a potential side effect of metformin. Metformin treatment significantly increased the abundance of the LPS-producing phylum Proteobacteria. In line, metformin increased the gut microbial production potential of LPS (KEGG M00080) and serum LPS levels, albeit without reaching significance (Figure S2G–I).

Taken together, metformin-induced microbiome effects are primarily characterized by enhanced production of the SCFA propionate and acetate.

2.3 | Metformin treatment reduces blood pressure

Since SCFA and blood pressure regulation are closely linked,^{17,19} we investigated blood pressure by radiotelemetry. dTGR-developed severe arterial hypertension exceeding 250 mmHg at the end of the trial (Figure 2A). Metformin treatment significantly decreased diastolic (DBP) and systolic blood pressure (SBP) beginning from treatment days 5 and 10, respectively (Figure 2A,E). The weekly mean BP, assessed using the area under the curves for SBP and DBP, was significantly lowered from week five onwards (Figure 2B–D,F–H). No significant differences in heart rate were observed with metformin treatment (Figure S3A–D). Notably, the mean DBP and SBP over the complete treatment period correlated significantly with fecal levels of acetate and propionate (Figure 2I,J, Figure S3E,F), indicating a link between increased SCFA

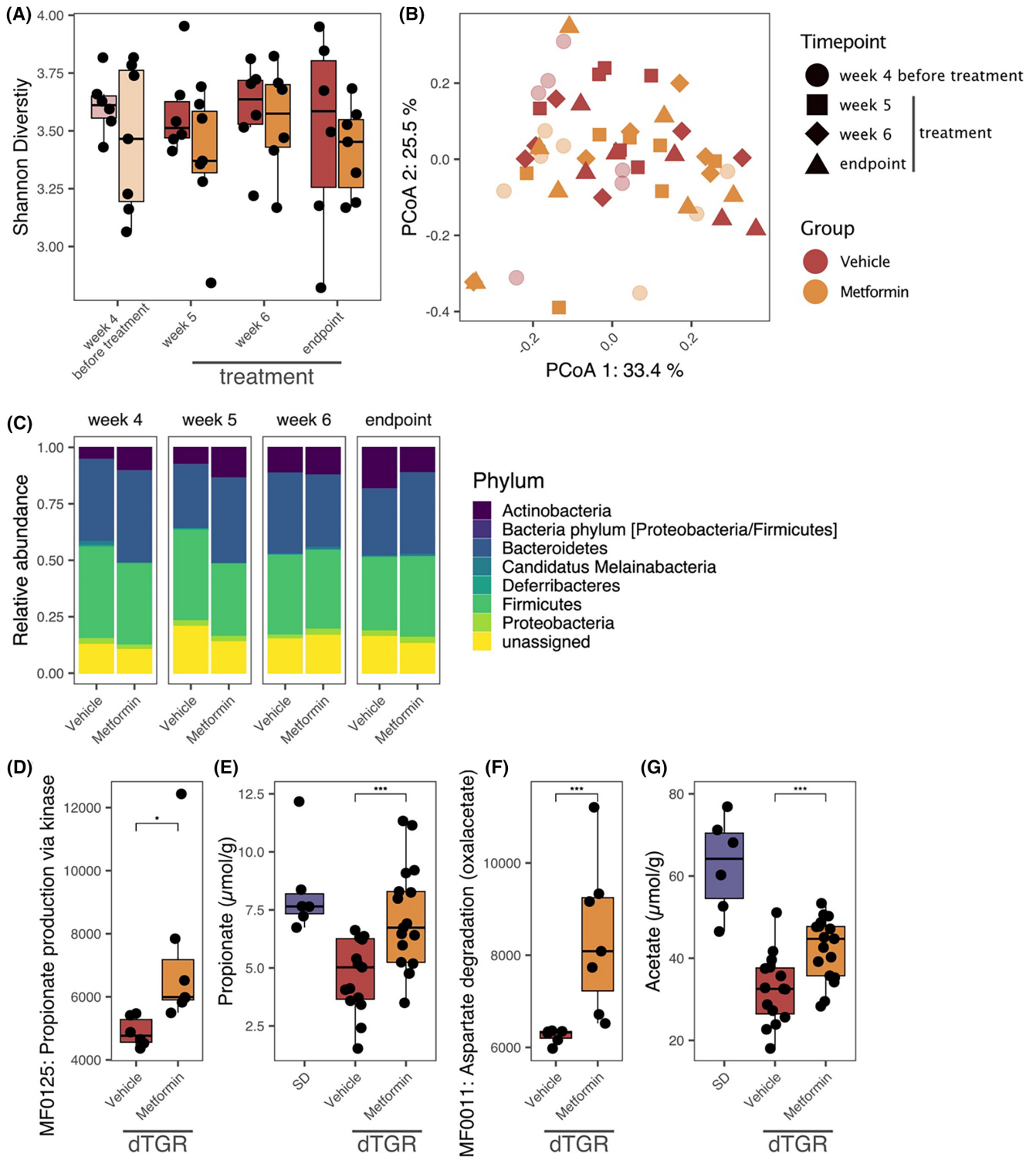


FIGURE 1 Metformin induces microbial short-chain fatty acid synthesis. Longitudinal shotgun metagenomic sequencing was conducted on fecal samples of metformin-treated (Metformin; $n = 7$) and vehicle-treated (Vehicle; $n = 6$) dTGR prior to treatment initiation (week 4 before treatment) and on consecutive weeks thereafter (week 5, week 6, and week 7 (endpoint)). (A) Alpha-diversity measured by Shannon index and (B) PCoA of beta diversity using Bray-Curtis dissimilarities were calculated (C) Microbiome taxonomic composition on phylum level across different timepoints. Gut microbial production potential of propionate (D); (MF0125) and acetate (F); (MF0011). Fecal SCFA concentrations measured by NMR at the endpoint (E), propionate; (G), acetate. A linear mixed model accounting for animal litter was used for gut microbial production potential of propionate and aspartate degradation and for propionate and acetate analyses; SD are shown for reference. The values are shown as raw data with each dot representing the data from one rat. Box plot represents median, 25th and 75th percentiles—interquartile range; IQR—and whiskers extend to maximum and minimum values. * $p < 0.05$, *** $p < 0.001$.

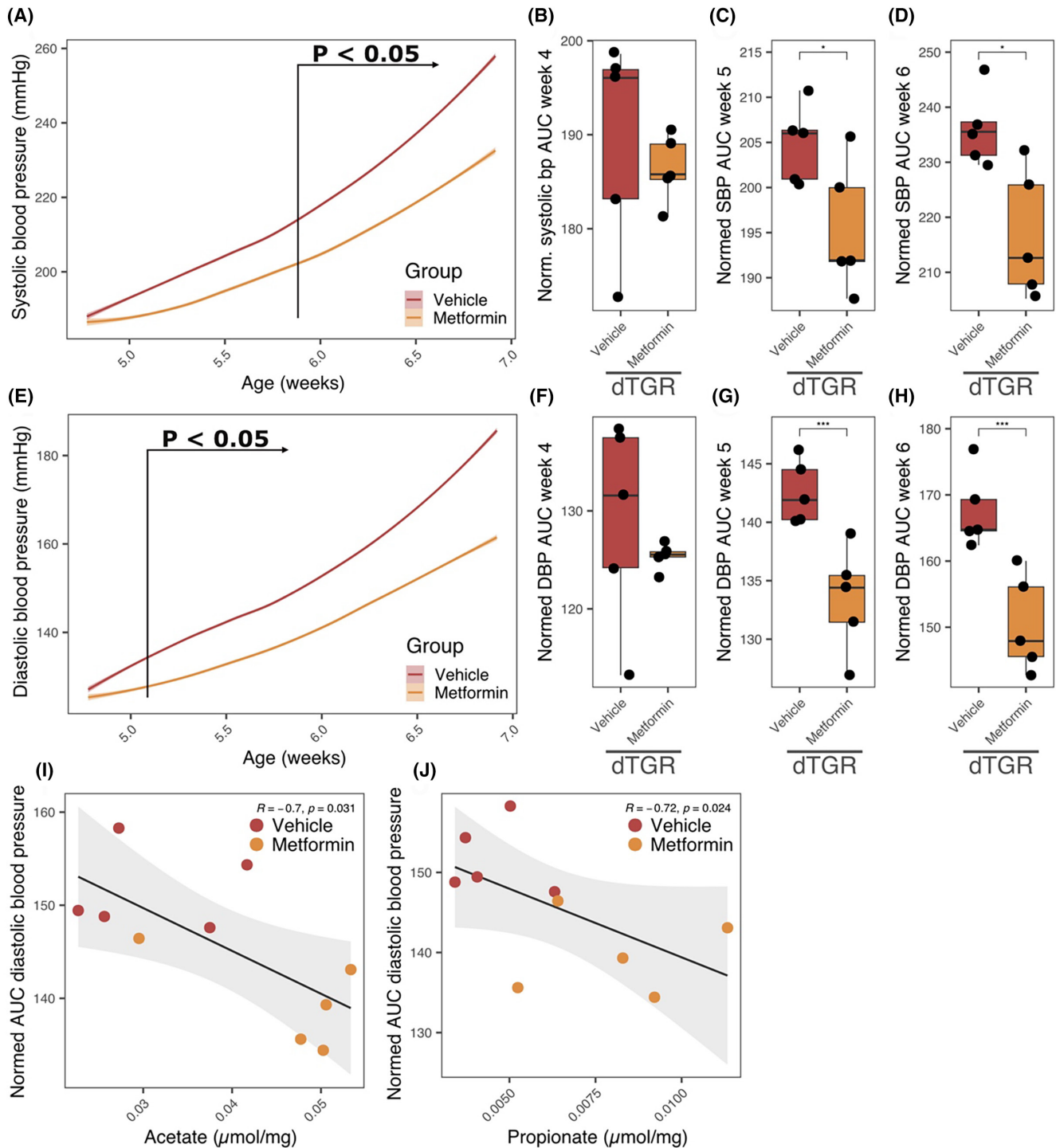


FIGURE 2 Metformin lowers blood pressure in hypertensive rats. Radiotelemetric blood pressure measurements of metformin-treated (Metformin; $n = 5$) and vehicle-treated (Vehicle; $n = 5$) dTGR. Treatment with 300 mg/kg metformin or vehicle was started at 4 weeks of age. (A) Analysis of systolic blood pressure over time. (B–D) Weekly mean systolic blood pressure quantified from the area under the curve (AUC) normalized to the number of measurements for week 4 (B), after treatment initiation, week 5 (C) and week 6 (D). (E–H) same for diastolic blood pressure. Correlations of mean diastolic blood pressure over the complete experimental time (analyzed as normed AUC) with fecal levels of acetate (I) and propionate (J). Spearman coefficients (R) and p values are shown, lines represent linear regression with a 95% confidence interval in gray. For analysis of blood pressure over lines represent mean values with a shaded 95% confidence interval, statistical analysis was performed using a rolling linear model. Mann–Whitney– U -test was used for normalized AUC. The values are shown as raw data with each dot representing one animal. B The box plot represents median, 25th and 75th percentiles—interquartile range; IQR—and whiskers extend from 5–95. percentile. * $p < 0.05$, *** $p < 0.001$.

production of the gut microbiome and improved blood pressure in metformin-treated dTGR.

2.4 | Metformin treatment effects on cardiac hypertrophy and function

We and others have investigated the relationship between SCFA, blood pressure, and cardiac remodeling in the past.^{19,20} Interestingly, metformin treatment in dTGR significantly increased the cardiac hypertrophy as assessed by echocardiography over time (Figure 3A) and heart weight-to-tibia ratio³⁶ at the endpoint (Figure 3B). Furthermore, the hypertrophy marker plasma B-type natriuretic peptide (BNP) was elevated in metformin-treated dTGR and closely correlated with the measured normalized heart weight (Figure S4A). Histological analysis revealed an enlarged cardiomyocyte cross-sectional area (CSA) in dTGR, which was unaffected by metformin (Figure 3D,F). Interstitial fibrosis quantified in WGA staining remained unchanged with metformin treatment (Figure 3E,F). In line, perivascular and interstitial fibrosis were unchanged in Sirius red staining (Figure S4B,C). We did not observe an overall strong pro-fibrotic phenotype in these litters of dTGR, in line, a comparable low grade of cardiac fibrosis was already noted in the model description.²⁶ This finding was also reflected in the similar expression of fibrosis-related genes collagen type I (*Col1*), collagen type IV (*Col4*), Fibronectin (*Fn1*), connective tissue growth factor (*Ccn2*), and transforming growth factor-beta (*Tgfb1*) (Figure S4D–H). To investigate the cardiac function in the context of the pro-hypertrophic effect of metformin, comprehensive functional phenotyping of the heart was employed using conventional and strain echocardiography. Data-driven PCA revealed clustering by treatment (Figure 3G), indicating apparent differences in cardiac function upon metformin treatment. Analysis of the treatment distinguishing component (PC2) showed that in addition to expected features like cardiac diameters, mainly the end-diastolic volume (EDV), the stroke volume (SV), and the cardiac output (CO) drove the separation (Figure S4I). Compromised ventricular filling, manifested by decreased EDV, is a hallmark of diastolic dysfunction. Metformin treatment increased the EDV (Figure 3H) and normalized the left ventricular filling pattern, as evidenced by a normal E/A ratio (Figure 3I). Notably, the increased EDV did not arise from a pathological ventricular dilatation. Measures of systolic function, including left ventricular ejection fraction and strain analyses, remained unaffected by metformin treatment (Figure 3J, Figure S4J–M). To investigate if the increase in BNP, EDV, and stroke volume was secondary to metformin treatment-induced intravascular volume

expansion, we analyzed body weight, urine output, and drinking volumes. However, neither body weight nor urine output and drinking volumes differed during the first days of metformin treatment (Figure S5A–C).

Overall, these alterations indicate improved cardiac function, as validated by increased SV and CO (Figure 3K, Figure S4M). Interestingly, fecal acetate levels correlated significantly with EDV (Figure S4N), while the correlation with propionate did not reach significance (Figure S4O).

Another hallmark of pathological cardiac remodeling in hypertension is the presence of inflammation. Flow cytometric analysis showed that the percentage of leukocytes among cardiac cells, which was increased by hypertension, was reduced by metformin treatment, although not statistically significant (Figure 3L). Similarly, metformin significantly lowered the gene expression of the heart failure-associated fetal myosin heavy chain isoform beta (*Myh7*) (Figure 3M).

Taken together, metformin improved heart function, leading to improved EDV, SV, and CO. Our data indicates that the stronger hypertrophic response might be attributable to an improved adaptive cardiac remodeling in response to hypertension in metformin-treated rats.

2.5 | Metformin treatment does not alter hypertensive renal and microvascular structure

dTGR show hallmarks of hypertensive kidney damage (Figure S6A–H). However, metformin treatment did not alter this damage, as assessed by blood urea nitrogen (BUN), plasma creatinine, urinary albumin/creatinine ratio, and leukocyte infiltration (Figure S6A–E). Furthermore, gene expression of the kidney damage marker NGAL (*Lcn2*) and fibrosis markers collagen type I (*Col1*) and transforming growth factor-beta (*Tgfb*) remained unchanged following metformin treatment (Figure S6F–H). The microvascular structure of the kidney, tongue, and eye was unaffected by metformin, as assessed by ex vivo micro-computer tomography (μ CT), indicated by unchanged vessel diameter and volume quantification (Figure S6I–K). Of note, in this independent cohort, we observed comparable effects of metformin on LV mass, EF, and EDV in the echocardiographic analysis (Figure S5D–F).

2.6 | Metformin ameliorates hypertensive cardiac inflammation

Since metformin leads to improved cardiac function with signs of lower inflammation and considering

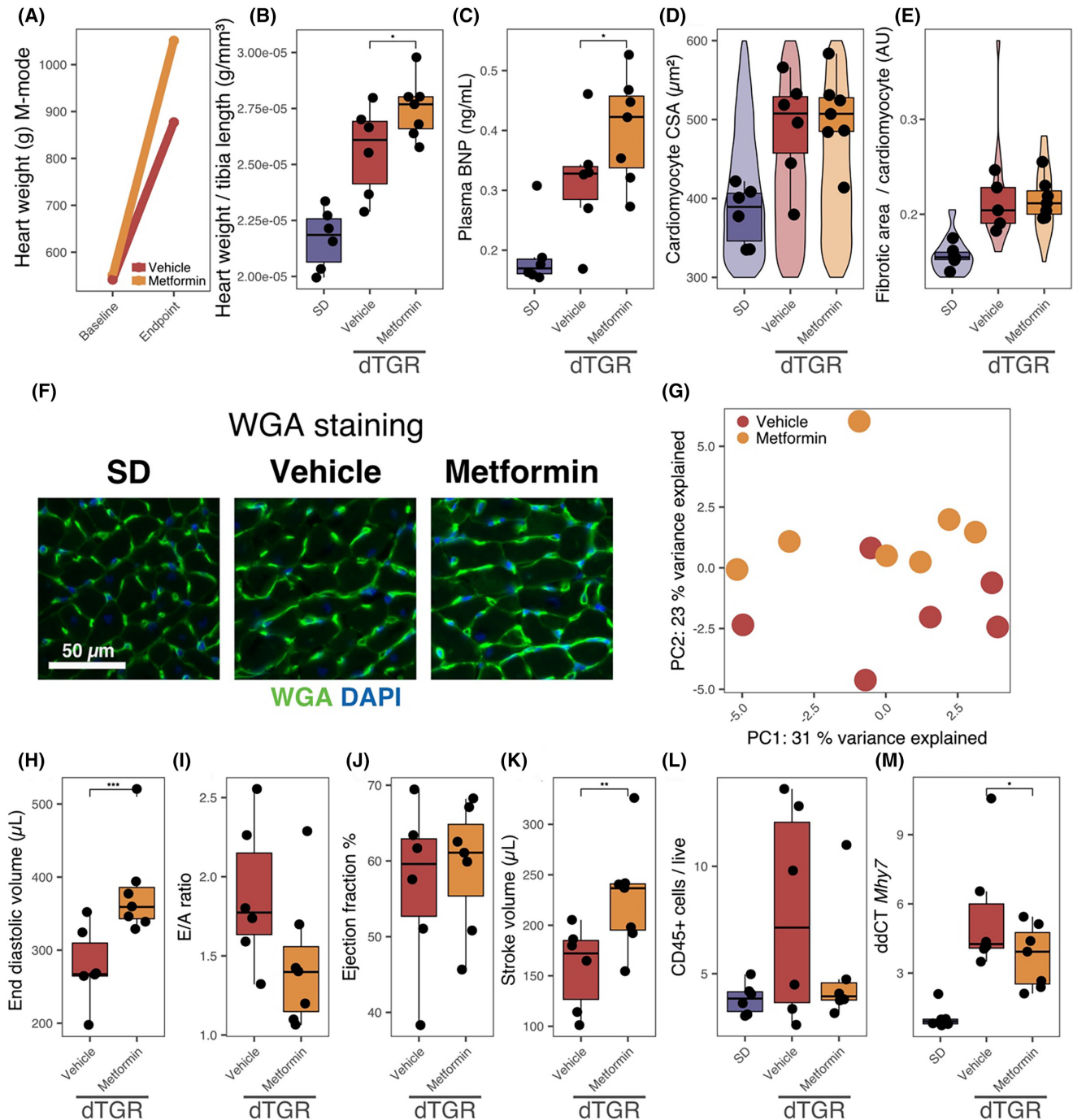


FIGURE 3 Metformin improves diastolic function in hypertensive rats. Hypertensive double transgenic rats (dTGR) were treated with metformin or vehicle. (A) Longitudinal echocardiography before the initialization of treatment (Baseline, week 4) and at the end of treatment (Endpoint, week 7) indicates a stronger hypertrophy in metformin-treated rats. (B) Confirmation using heart weight (normalized to tibia length³) and (C) plasma BNP levels. (D) Cardiomyocyte hypertrophy and (E) Interstitial cardiac fibrosis was assessed using WGA Staining (F) representative pictures of WGA staining. (G) PCA of all echocardiographic features. Diastolic and systolic function was further analyzed at the endpoint. (H) End-diastolic volume (EDV), (I) E/A, (J) left ventricular ejection fraction (EF), and (K) stroke volume (SV) were analyzed. (L) Cardiac inflammation was quantified by flow cytometry as CD45+ cells (leukocytes) in percent of live cells. (M) Cardiac *Mhy7* mRNA expression was assessed by qPCR. A linear mixed model accounting for animal litter was used for all comparisons of metformin treatment with vehicle; SD are shown for reference. The values are shown as raw data with each dot representing the data from one rat. Box plot represents median, 25th and 75th percentiles—interquartile range; IQR—and whiskers extend from 5–95. percentile. * $p < 0.05$, ** $p < 0.01$, *** $p < 0.001$.

the anti-inflammatory effects of SCFA, we performed comprehensive immune phenotyping of the heart, the kidney, and the spleen as a systemic lymphoid organ (Figure S7A, gating strategies Figure S8A–D). Our analysis revealed an inflammatory signature in the hearts of vehicle-treated dTGR as compared to SD across various innate and adaptive immune populations (Figure 4A,B, Figure S9A–L). Metformin treatment shifted the immune phenotype towards SD (Figure 4A,B). A detailed analysis of the cardiac immune cell composition demonstrated anti-inflammatory changes within macrophage populations with metformin treatment (Figure 4C–G). Metformin decreased macrophage and monocyte infiltration into the heart (Figure 4C,D). Cardiac infiltrating monocytes exhibited a less pro-inflammatory³⁷ (His48+) phenotype with metformin treatment (Figure 4E). Furthermore, metformin reduced cardiac pro-inflammatory M1-like macrophages (CD11b/c^{high}CD86+; Figure 4F), while cardiac regulatory M2-like macrophages (CD11b/c^{low}CD163+) were increased (Figure 4G). In addition, metformin restored normal cardiac T cell abundance (T cells; CD3+; Figure S9A), reduced cardiac gamma delta T cells (gdT; gdTCR+ T cells; Figure S9D) and regulatory T cells (Treg; FoxP3+ T helper [Th, CD3+ CD4+ CD8–]; Figure S9E). In conjunction with this, cardiac pro-inflammatory T helper cell subsets such as Th17-like Treg (RORgt+ Tbet– Treg) and Th17 cells (RORgt+ Tbet– FoxP3– Th cells), known for their role in mediating hypertensive damage,³⁸ were reduced albeit not significantly (Figure 4H,I). Interestingly, the levels of infiltrating macrophages correlated significantly with acetate and propionate levels (Figure 4J,K).

Systemic immune signatures assessed in the spleen were not altered (Figure S7B). In line with the unaffected kidney phenotype, metformin did not improve renal inflammation (Figure S7C).

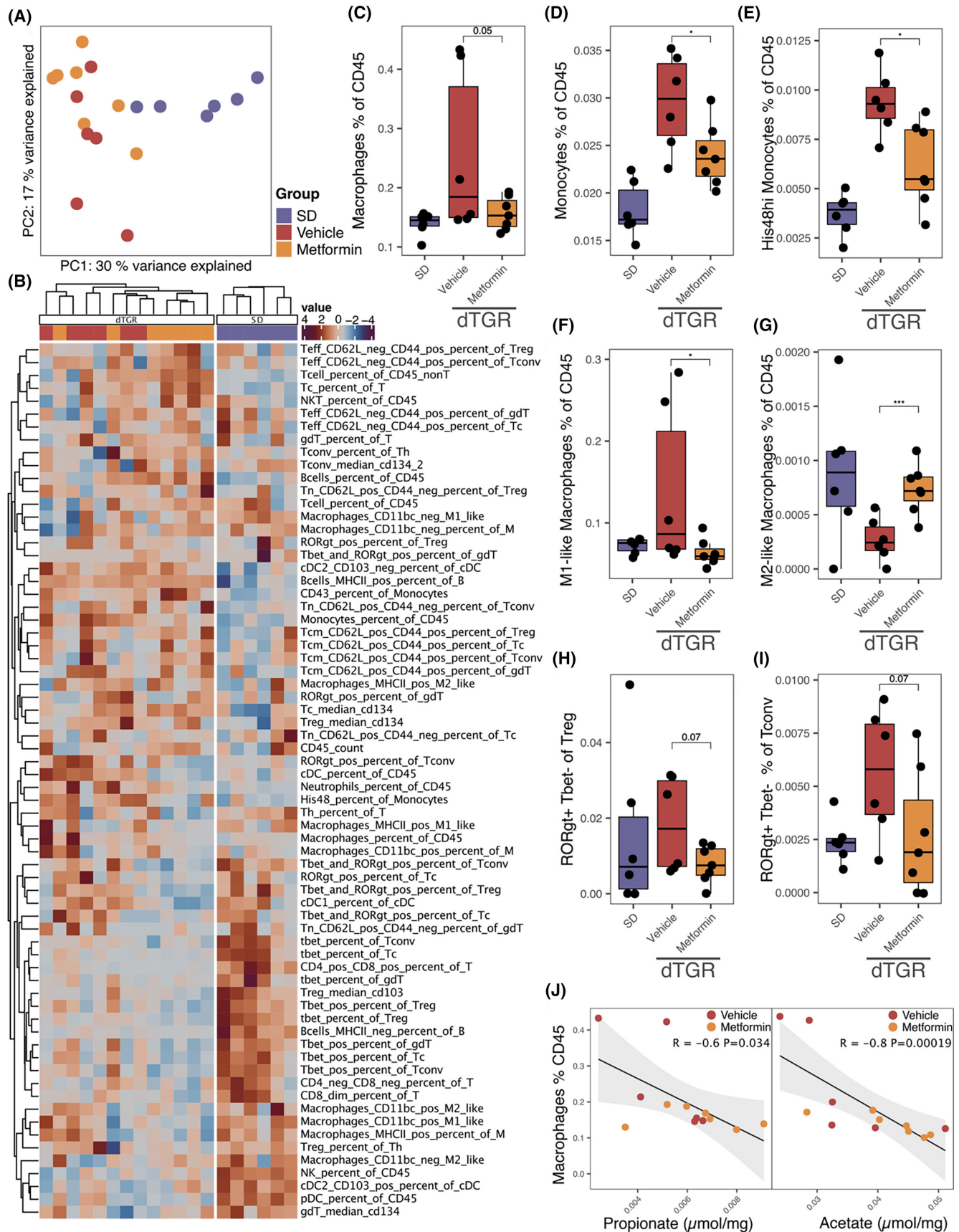
In summary, our data indicates an improved cardiac inflammatory response in metformin-treated dTGR. Macrophages were most affected by metformin treatment and showed a negative correlation with fecal propionate

and acetate levels. Since inflammation is a hallmark of pathological cardiac remodeling, the observed immune response may explain the observed improvements in cardiac function.

2.7 | Short-chain fatty acid modulate M1-like but not M2-like macrophages in vitro

The beneficial effects of metformin on SCFA production as well as on cardiac macrophage infiltration led us to investigate the effect of SCFA on macrophage polarization. We have previously shown that the protective effects of propionate can be explained in particular by an anti-inflammatory modulation of T cells.¹⁹ Here, we hypothesized that SCFA affects the polarization of macrophages. Murine bone marrow-derived macrophages (BMDMs) were polarized in vitro towards M1-like (LPS) and M2-like (IL-4 + IL-13) phenotypes and treated with 1 mM of acetate, propionate, and butyrate. Propionate and acetate altered the expression of key M1-like macrophage marker genes such as inducible nitric oxide synthase (*Nos2*), cyclooxygenase-2 (*Cox2*), interleukin-6 (*Il6*), C-C Motif Chemokine Ligand 5 (*CCL5*), IL-1 β (*Il1b*), NLRP3 (*Nlrp3*), and tumor necrosis factor (*Tnf*) (Figure 5A,B). Interestingly, even under M2 conditions, we observed an inhibition of the M1 signature by SCFA treatment. Butyrate, which was not regulated by metformin treatment, showed the weakest effect on M1-like polarization and even lead to an induction of *CCL5*. Under M2 conditions, acetate lead again to a reduced polarization (Figure 5A,C). Propionate and butyrate treatment showed more intermediate effects with an induction of several marker genes and an inhibition of others (Figure 5A,C). However, the observed effects (log₂FC) were comparable smaller on M2-like macrophages compared to M1-like macrophages. To validate this, we tested whether the effect on M1-like macrophages was also achieved with a lower dose of 100 μ M of the respective SCFA.

FIGURE 4 Metformin ameliorated cardiac hypertensive inflammation. Cardiac immune cells from hypertensive double transgenic rats (dTGR) were treated with metformin or vehicle and were analyzed by flow cytometry. (A) PCA of cardiac immune cells. (B) Heatmap showing z-scored/transformed immune cell abundances and K-means clustering of dTGR samples. SD is shown as a reference. (C) Macrophages (CD45+ CD3– CD161– RP1– CD68+), (D) monocytes (CD45+ CD3– CD161– RP1– CD68– CD45R– RT1b– CD4+), (E) His 48^{high} monocytes, (F) M1-like (CD11b/c^{high} CD86+) macrophages, (G) M2-like (CD11b/c^{low} CD163+) macrophages, (H) RORgt+ regulatory T cells (Treg, CD45+ CD3+ gdTCR– CD8– CD4+ FoxP3+ RORgt+ Tbet–), and (I) RORgt+ conventional T cells (CD45+ CD3+ gdTCR– CD8– CD4+ FoxP3– RORgt+ Tbet–) are shown as boxplots. (J) Correlations of macrophages with fecal acetate and propionate levels. Spearman coefficients (*R*) and *p* values are shown, lines represent linear regression with a 95% confidence interval in gray. A linear mixed model accounting for animal litter was used for all comparisons of metformin treatment with the vehicle; SD are shown for reference. The values are shown as raw data with each dot representing the data from one rat. Box plot represents median, 25th and 75th percentiles—interquartile range; IQR— and whiskers extend from 5–95. percentile. **p* < 0.05, ****p* < 0.001.



Consistent with the signature of 1 mM SCFA, propionate, and acetate showed again the strongest effects (Figure S10).

Taken together our in vitro data suggest a functional link of microbially-produced SCFA to macrophage abundance and polarization in metformin-treated dTGR.

3 | DISCUSSION

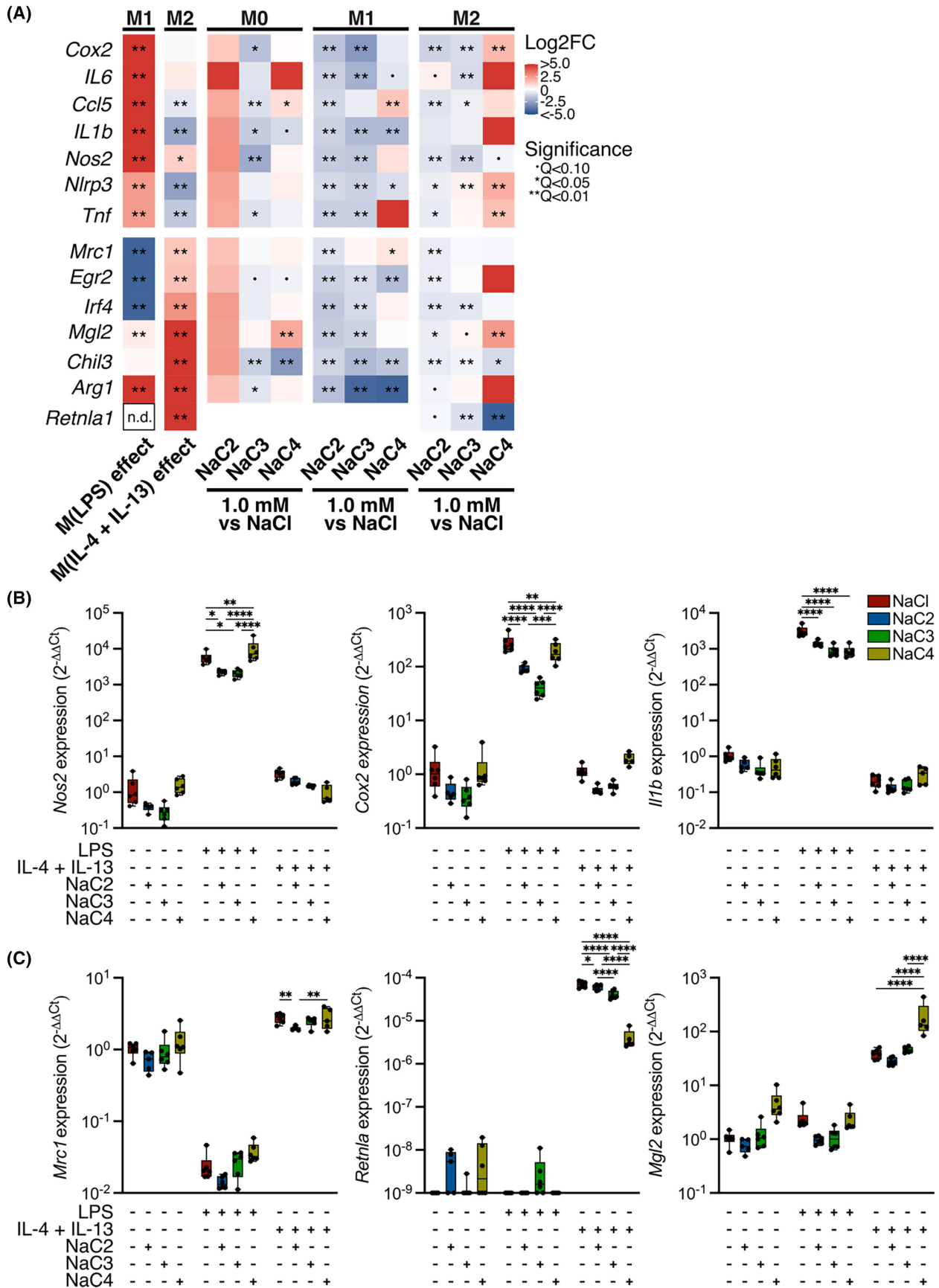
Given the role of metformin in preventing cardiovascular disease under diabetic conditions, we aimed to investigate the effects of metformin on cardiovascular damage in hypertension in the absence of diabetes. In line with findings from human cohorts,^{14–16} metformin induced a functional shift in the gut microbial metabolite production by increasing the production of the SCFA acetate and propionate. Furthermore, metformin treatment significantly lowered DBP and SBP. Despite a more pronounced cardiac hypertrophy, metformin treatment reduced cardiac inflammation and improved cardiac function. A hallmark of the improved cardiac immune phenotype was the shift in macrophage subpopulations towards less inflammatory subtypes, which was reproduced in vitro in SCFA-treated BMDM. Apart from cardioprotective effects, metformin treatment did not overtly affect other hypertensive end-organs such as the kidney. Taken together, our data indicates a cardioprotective effect of metformin treatment, which can at least in part be explained by beneficial microbial shifts.

First, we aimed to confirm the known microbiome-dependent effects of metformin in our study. Since 1984, it is known that metformin exhibits no glucose-lowering effects after intravenous administration.^{11,12} Interestingly, approximately 70% of the orally administered metformin gets excreted unmetabolized via feces and urine.¹⁰ Microbiome analyses of large human diabetic cohorts have uncovered that metformin induces a microbiome signature initially believed to be a consequence of type 2 diabetes.¹⁴ This signature was mainly characterized by an increased gut microbial SCFA production potential, which correlated with metformin plasma levels, but also an increase in LPS-producing bacteria. The effect of metformin on SCFA production could be confirmed in other human studies using metabolomics approaches.^{13,15,16} Interestingly, the aforementioned studies also confirmed the increase in LPS-producing bacteria.¹⁵ Using shotgun sequencing, we observed an increase in SCFA-associated pathways at early time points and a loss of this signature with disease progression. However, fecal SCFA levels

remained elevated following metformin at the end of the study. Similar to the studies in human, we found an increase in LPS, LPS-producing bacteria, and production pathways. However, most of these findings did not reach significance in our study.

Recently, metformin treatment of spontaneous hypertensive rats (SHR) was shown to improve blood pressure and reduce cardiac hypertrophy.⁵ Although the same metformin dose was used, the authors used another rat model with a different and more heterogeneous genetic background, as well as a more moderate, longer disease course and thus a longer metformin treatment duration. Previous studies have shown an improvement of endothelial-dependent vasorelaxation in diabetic rats treated with metformin.³⁹ These effects are in part also recapitulated in patients.⁴⁰ In line, the authors of the above-mentioned SHR publication suggest various mechanisms including reduced oxidative stress as the reason for the reduction in blood pressure. The metformin-induced increase in microbiome-derived SCFA in our study provides an alternative explanation for the antihypertensive effect by metformin treatment. In our study, we observed a combination of higher CO with lower BP, which indicates a lower systemic vascular resistance. As shown by others, SCFA bind to G-protein-coupled receptors (GPR) from the olfactory receptor group (OLFR78, GPR41, GPR43, and GPR109a), thereby mediating effects of SCFA such as acetate and propionate in vascular cells.¹⁷ Pluznick and colleagues have performed multiple compelling in vivo studies demonstrating that SCFA, particularly acetate, binds to G-protein-coupled receptors 41 and 43 (GPR41/43), leading to vasodilation and subsequently reducing systemic vascular resistance.^{17,41–43} As a result, an acute decrease in BP can be observed after intra-peritoneal injection of acetate.⁴² Blood pressure modulation by SCFA via orphan GPR has been described in several animal models and are an intriguing explanation for the blood pressure effect observed in both SHR and dTGR. Moreover, both the cardiometabolic effects of metformin as well as SCFA effects on metabolism (independent of metformin) have recently been explained

FIGURE 5 SCFA influences macrophage polarization. Mouse bone-marrow derived macrophages (BMDM) were differentiated towards an M1-like phenotype using LPS and M2-like phenotype using IL-4 and IL-13 for 24 hrs in the presence of 1 mM sodium acetate (NaC2), sodium propionate (NaC3), sodium butyrate (NaC4) or sodium chloride (NaCl). (A) Heatmap showing log₂-transformed fold changes (log₂FC) of typical marker genes for M1-like differentiation (cyclooxygenase-2 (*Cox2*), interleukin (IL)-6 (*Il6*), chemokine (C-C motif) ligand 5 (*Ccl5*), IL-1β (*Il1b*), inducible nitric oxide synthase (*Nos2*), NLRP3 (*Nlrp3*), tumor necrosis factor (*Tnf*)) and M2-like differentiation (resistin-like molecule alpha (*Rtnla1*), arginase-1 (*Arg1*), chitinase-like 3 (*Chil3*), macrophage galactose-type lectin 2 (*Mgl2*), interferon regulatory factor 4 (*Irf4*), early growth response protein 2 (*Egr2*), and Mannose receptor C-type 1 (*Mrc1*)). Statistical comparison with BH-FDR corrected Mann–Whitney-*U* tests, •*Q* < 0.1, **Q* < 0.05, ***Q* < 0.01. (B) Boxplots showing gene abundance of *Nos2*, *Cox2*, and *Il1b* as M1 markers. (C) Boxplots showing gene abundance of *Mrc1*, *Rtnla*, and *Mgl2* as M2 markers. Dots indicate replicates (*n* = 6). Statistical comparisons were performed using 2-way ANOVA with the Tukey post hoc test. **p* < 0.05, ***p* < 0.01, ****p* < 0.001, *****p* < 0.001.



by a modulation of AMPK activity.⁴⁴ Although our study did not focus on AMPK, AMPK-dependent effects in the presence of metformin and metformin-induced SCFA

may have played an additional role in the observed cardiovascular protection. Additionally, SCFA have been shown to fuel mitochondrial respiration, which may

contribute to the metabolic phenotype observed in cardiac tissue of SHR.⁴⁵ Taken together, our findings emphasize the significance of microbiome-mediated effects as an additional explanation for the observed cardiovascular protection by metformin in hypertensive non-diabetic conditions. Future studies should consider the potential metabolic effects of SCFA when investigating metformin.

A paradoxical observation is the increased cardiac hypertrophy in metformin-treated dTGR despite indications of an improved cardiac function. We have seen previously in the same model that despite improved blood pressure control, as in our study, dTGR can still exhibit cardiac hypertrophy.³¹ In addition, previous immunosuppressive treatment regimens in this model have shown that effects on cardiac hypertrophy and lowered blood pressure are not necessarily linked.²⁷ Nevertheless, we observed improved diastolic and preserved systolic functions, resulting in higher cardiac output. The preserved systolic function suggests that the augmented EDV is not a consequence of dilated ventricles, which typically manifests as impaired systolic function. In addition, these changes were accompanied by a profound improvement in the cardiac inflammatory response. Taking the lower cardiac inflammation into account, the higher heart weight might be a sign of adaptive remodeling towards the extremely high blood pressure. Even under metformin treatment, dTGR had a mean SBP of 230 mmHg on the last day of the experiment. This is also a key difference compared to the above-mentioned SHR model. As previously published,⁴⁶ plasma BNP was most reflective of cardiac hypertrophy in dTGR, as it closely correlated with the normalized heart weight. Interestingly, in hypertensive patients left ventricular mass index correlates with plasma BNP within the normal range.^{47,48}

Of note, we did not observe differences in cardiac fibrosis. We observed overall little cardiac fibrosis compared to wild-type SD rats, confirming findings from earlier reports.²⁶ The term “hidden fibrosis” was recently introduced by Travers et al.⁴⁹ to describe cardiac fibrosis that is undetectable by histological methods and can only be identified through gene expression and proteomic analyses. In their study, the authors demonstrated that cardiac fibrosis induced by deoxycorticosterone acetate (DOCA) plus uninephrectomy, compared to uninephrectomy alone, was not evident in histological examinations but was revealed through gene expression and proteomic approaches. Moreover, the effects of histone deacetylase (HDAC) inhibition were also only detectable via gene expression and proteomics. In the present study, no alterations in histological fibrosis or gene expression of pro-fibrotic genes were observed

following metformin treatment. However, the possibility of hidden fibrosis, detectable by proteomic analysis, cannot be excluded. Further research is required to address this aspect, as it is beyond the scope of the current investigation.

Inflammation is characteristic of pathological cardiac remodeling^{50–52} and cardiac dysfunction,⁵³ thus contributing to adverse outcomes.⁵⁴ Macrophages have been implicated in hypertensive organ damage.^{55,56} Here, metformin reduced not only cardiac macrophages in dTGR, but also monocyte-like cells, which most likely representing recently infiltrated monocytes. Overall, macrophage depletion was shown to not only leading to improved cardiac remodeling, but also reduced blood pressure.⁵⁶ Furthermore, we observed a switch from M1-like towards M2-like phenotypes. While M1-like macrophages have been demonstrated to drive cardiovascular damage, M2-like macrophages have been shown to confer protection.⁵⁷ Interestingly, we could show that acetate and propionate influenced the differentiation of M1-like M (LPS) macrophages *in vitro*. Our data falls in line with reports on the role of SCFA in macrophage differentiation.^{58,59} The cellular mode-of-action for SCFA in metformin-treated dTGR is beyond the scope of this study. SCFA have been shown to bind to GPR such as GPR41, GPR43, and GPR09a as well as to act as HDAC inhibitors.^{58,59} Interestingly, we observed effects – although not statistically significant – on ROR γ t+ IL17A-producing Th17 and regulatory T cells. Multiple publications have shown that SCFA directly influence Th17 differentiation.^{60,61} Therefore, these immune cell types might be of interest for future investigations on metformin effects in cardiovascular disease models.

It is worth to mention that blood pressure, cardiac remodeling, and inflammation are closely linked in hypertension. While we suggest inflammation as a mediator of the metformin and SCFA effects on the cardiac phenotype, improvement of cardiac function might as well be a reflection of the blood pressure-lowering effects of SCFA and metformin discussed above. In line, the normalization of blood pressure levels with Valsartan and Aliskiren in dTGR is linked to less inflammation.²⁹ However, metformin treated animals still had SBP levels well above 200 mmHg during the last week of treatment. Unfortunately, the interplay of inflammation, blood pressure, and cardiac remodeling cannot be disentangled with the current data and requires further investigation.

While our study describes a contribution of the gut microbiota to the observed metformin effects on blood pressure and cardiac remodeling, their relevance in comparison to potentially direct effects of metformin on

cardiovascular cells remain to be elucidated by complex fecal microbiome transfer experiments that go beyond the scope of the current study. In addition, the sample sizes for some analyses were small, although the phenotypes observed were very consistent across the three experimental runs presented here. Lastly, we only analyzed male rats in this study. Sex bias in preclinical research is a prevalent problem.⁶² However, female dTGR have a protected phenotype⁶³ which mostly masks the smaller treatment effects. Future studies are needed to confirm our findings in cardiovascular animal models better suited to analyze the female sex.

In summary, the study provides further evidence that metformin mediates cardiovascular protection beyond its anti-diabetic effects in severe Ang II-induced hypertension. Metformin effects on the intestinal microbiome, in particular the increased production of SCFA, appear to be partially responsible for the effects on blood pressure, inflammatory response, and cardiac function.

4 | MATERIALS AND METHODS

The data that support the findings of this study are available from the corresponding author upon reasonable request. Full material and methods are available in the online supplementary materials.

4.1 | Animal ethics and housing

All experiments were performed in accordance with the German/European law for animal protection. Experimental protocols were approved by the local ethics board (G0019/21). All animals were housed in the animal facility of the Max-Delbrück-Center for Molecular Medicine (MDC). Animals had constant access to a chow diet (V1324-300, Ssniff GmbH, Soest Germany) and tap water ad libitum and were maintained on a constant 12:12 h day: night cycle.

4.2 | Animal protocols

In the animal facility of MDC, female homozygous human renin and homozygous male human angiotensinogen rats were mated to obtain dTGR offspring. As female rats developed a comparably weaker phenotype,⁶³ only male offspring were used. Four-week-old male dTGR were randomized, accounting for litter, into oral treatment with metformin (metformin hydrochloride) or vehicle (magnesium chloride, MgCl₂) control, both obtained from Sigma-Aldrich (Merck, Darmstadt,

Germany). Treatment was performed for 3 weeks, and the animals were sacrificed at 7 weeks of age. Rats and water bottles were weighed two times per week. Metformin and vehicle concentration in the drinking water were adjusted to 1.811 mmol/g body weight/day and 0.9055 mmol/g body weight/day, respectively. Rats were housed in cages of one to two rats and the mean body weight was used to determine the dosage. Animals were used for (i) an immune cohort undergoing 6 h of metabolic cages, echocardiography, and immune analysis at the endpoint (7× Metformin, 6× Vehicle); (ii) a telemetry cohort which had radiotelemetric blood pressure device (Data Science International, St. Paul, MN, USA), implanted (5× Metformin, 5× Vehicle); (iii) a μCT cohort that underwent perfusion with cast material to analyze microvasculature at the endpoint (5× Metformin, 4× Vehicle). Wild-type Sprague–Dawley (SD) rats from in-house breeding (MDC) were used to compare the immune phenotype at the endpoint. At 7 weeks of age animals were sacrificed and organs were collected. For the immune and μCT cohorts, animals were sacrificed in isoflurane narcosis (2%–2.5%) and analgesia with 0.05 mg/kg bodyweight buprenorphine. After the abdomen was opened the thorax was accessed through the diaphragm, the heart was punctured to draw blood, the animals were perfused via the left ventricle with physiological saline solution. Urine was collected from bladder punctures when possible. For the μCT cohort, animals were subsequently perfused with Vascupaint Silicone Rubber Injection Compounds (MediLumine, Montreal, Canada).

Spleen, one kidney, and half of the sagittal cut heart were collected for flow cytometry. For RNA analysis tissue pieces were snap frozen in liquid nitrogen. For histology, tissues were placed in PBS-buffered 4% paraformaldehyde (PFA) solution and kept at 4°C.

Animals from the telemetry cohort were euthanized by decapitation in isoflurane narcosis.

For macrophage differentiation experiments primary cells from wild-type C57BL6/J mice (in-house breeding, MDC) were used ($n=3$ mice, three independent experiments).

4.3 | Statistical analyses

Endpoint data was analyzed by nested model comparisons, one with only the littermate status and another one additionally incorporating the group label. The models were compared using a likelihood ratio test and $p < 0.05$ was considered statistically significant. For reference, analysis from SD rats is shown for endpoint data in the immune cohort.

PCoA (Figure 1B) shows β -diversity by Bray–Curtis dissimilarity. For the cuneiform plot in Figure S1 effect sizes were calculated using standardized non-parametric effect size metric (Cliff's Delta) and tested with Mann–Whitney-*U* Test and Bonferroni FDR correction.

Blood pressure differences were assessed by a rolling linear model; AUC were standardized to the number of measurements (normed AUC) and compared by Mann–Whitney-*U* test (Figure 2B–D,F,G, Figure S2B–D). Correlations of several parameters with SCFA acetate and propionate were analyzed using non-parametric Spearman correlation and displayed as a linear regression and 95% confidence interval (Figures S2 and S4, Figure 4). All PCAs (Figures 3G and 4C,D) were computed using Euclidean distance. Unless otherwise stated, analysis was performed in R (v4.1.2) with the following packages: tidyverse, performance, slider, vegan, ggpubr, orddom, tidyHeatmap, and ComplexHeatmap packages and visualized using ggplot2. Macrophage differentiation assays were analyzed in GraphPad Prism (GraphPad) by two-way ANOVA and Tukey's post-hoc test. Adjusted *p*-values below 0.05 were considered significant.

Results of all statistical analyses were displayed as **p* < 0.05, ***p* < 0.01, ****p* < 0.001, and *****p* < 0.0001.

AUTHOR CONTRIBUTIONS

Moritz I. Wimmer: Investigation; methodology; software; formal analysis; visualization; data curation; conceptualization; writing – original draft. **Hendrik Bartolomaeus:** Investigation; formal analysis; methodology; conceptualization; visualization; writing – original draft. **Harithaa Anandakumar:** Formal analysis; software; validation; writing – review and editing. **Chia-Yu Chen:** Formal analysis; visualization. **Valentin Vecera:** Investigation. **Sarah Kedziora:** Investigation; validation. **Sakshi Kamboj:** Writing – review and editing; investigation. **Fabian Schumacher:** Formal analysis; investigation; methodology; writing – review and editing. **Sidney Pals:** Investigation. **Ariana Rauch:** Software; investigation; methodology; writing – review and editing. **Jutta Meisel:** Investigation. **Olena Potapenko:** Investigation. **Alex Yarritu:** Investigation. **Theda U. P. Bartolomaeus:** Investigation. **Mariam Samaan:** Investigation. **Arne Thiele:** Validation. **Lucas Stürzbecher:** Investigation. **Sabrina Y. Geisberger:** Investigation; methodology. **Burkhard Kleuser:** Resources. **Peter J. Oefner:** Resources; writing – review and editing. **Nadine Haase:** Project administration. **Ulrike Löber:** Software; formal analysis; methodology; data curation. **Wolfram Gronwald:** Investigation; formal analysis; writing – review and editing; methodology. **Sofia K. Forslund-Startceva:** Conceptualization; funding acquisition; writing – review and editing; resources. **Dominik N. Müller:** Writing

– review and editing; funding acquisition; conceptualization; resources. **Nicola Wilck:** Conceptualization; funding acquisition; project administration; resources; methodology; supervision; writing – original draft.

ACKNOWLEDGMENTS

We thank Gudrun Koch, Melanie Röhr, Gabi N'diaye, Jana Czychi, Sina-Celine Stübler, and Daniel Herrmann for their excellent technical assistance. We thank Patrick Lange, Martin Taube, Reika Langanki, and Hanna Napieczynska, PhD from the Preclinical Research Center of the MDC for performing clinical chemistry, echocardiography, radio telemetry, and μ CT, respectively. Open Access funding enabled and organized by Projekt DEAL.

FUNDING INFORMATION

NW is supported by the European Research Council (ERC) under the European Union's Horizon 2020 research and innovation program (852796) and by a grant from the Corona-Stiftung, Deutsches Stiftungszentrum, Essen, Germany (S199/10080/2019). SKFS, DNM, and NW were supported by the Deutsche Forschungsgemeinschaft (DFG, German Research Foundation) Projektnummer 394046635 (CRC 1365; project A01) and DFG Projektnummer 437531118 (CRC 1470; A05 SKFS, A06 DNM, and A10 NW). DNM and SKFS were supported by the German Centre for Cardiovascular Research (DZHK, 81Z0100106). MIW was supported with an MD doctoral scholarship from the DZHK. NW, HB, DNM, WG, and PJO were supported by the BMBF (The Federal Ministry of Education and Research), Foerderkennzeichen 01EJ2202A, 01EJ2202D, and 01EJ2202B (TAhRget consortium). HB was supported by the BMBF, Foerderkennzeichen 13N16386 (QEED consortium). This study was funded by the DFG Projektnummer 394046635 (CRC 1365 A01). Deutsche Forschungsgemeinschaft and Deutsches Zentrum für Herz-Kreislaufforschung.

CONFLICT OF INTEREST STATEMENT

The authors have nothing to disclose.

DATA AVAILABILITY STATEMENT

The data that support the findings of this study are available from the corresponding author upon reasonable request.

ORCID

Moritz I. Wimmer  <https://orcid.org/0009-0004-5793-0249>

Hendrik Bartolomaeus  <https://orcid.org/0000-0003-4288-3828>

Harithaa Anandakumar  <https://orcid.org/0009-0000-3326-5126>

Chia-Yu Chen  <https://orcid.org/0000-0003-1765-7132>
 Valentin Vecera  <https://orcid.org/0009-0002-9969-1827>
 Sarah Kedziora  <https://orcid.org/0000-0003-0124-2557>
 Sakshi Kamboj  <https://orcid.org/0000-0001-9618-012X>
 Fabian Schumacher  <https://orcid.org/0000-0001-8703-3275>
 Ariana Rauch  <https://orcid.org/0000-0002-5152-5830>
 Olena Potapenko  <https://orcid.org/0000-0002-4397-568X>
 Alex Yarritu  <https://orcid.org/0000-0002-1724-0559>
 Theda U. P. Bartolomaeus  <https://orcid.org/0000-0002-5156-7184>
 Mariam Samaan  <https://orcid.org/0009-0008-5924-3732>
 Arne Thiele  <https://orcid.org/0000-0003-0786-2239>
 Sabrina Y. Geisberger  <https://orcid.org/0000-0001-6477-1312>
 Burkhard Kleuser  <https://orcid.org/0000-0002-1888-9595>
 Peter J. Oefner  <https://orcid.org/0000-0002-1499-3977>
 Nadine Haase  <https://orcid.org/0000-0003-0727-1738>
 Ulrike Löber  <https://orcid.org/0000-0001-7468-9531>
 Wolfram Gronwald  <https://orcid.org/0000-0003-3646-0060>
 Sofia K. Forslund-Startceva  <https://orcid.org/0000-0003-4285-6993>
 Dominik N. Müller  <https://orcid.org/0000-0003-3650-5644>
 Nicola Wilck  <https://orcid.org/0000-0003-3189-5364>

REFERENCES

1. ElSayed NA, Aleppo G, Aroda VR, et al. 9. Pharmacologic approaches to glycemic treatment: standards of Care in Diabetes-2023. *Diabetes Care*. 2023;46:S140-S157. doi:10.2337/dc23-S009
2. Monami M, Candido R, Pintaudi B, Targher G, Mannucci E, SID-AMD joint Panel for Italian Guidelines on Treatment of Type 2 Diabetes. Effect of metformin on all-cause mortality and major adverse cardiovascular events: An updated meta-analysis of randomized controlled trials. *Nutr Metab Cardiovasc Dis*. 2021;31:699-704. doi:10.1016/j.numecd.2020.11.031
3. Campbell JM, Bellman SM, Stephenson MD, Lisy K. Metformin reduces all-cause mortality and diseases of ageing independent of its effect on diabetes control: a systematic review and meta-analysis. *Ageing Res Rev*. 2017;40:31-44. doi:10.1016/j.arr.2017.08.003
4. Yang JY, Liu MJ, Lv L, et al. Metformin alleviates irradiation-induced intestinal injury by activation of FXR in intestinal epithelia. *Front Microbiol*. 2022;13:932294. doi:10.3389/fmicb.2022.932294
5. Li J, Minćzuk K, Massey JC, et al. Metformin improves cardiac metabolism and function, and prevents left ventricular hypertrophy in spontaneously hypertensive rats. *J Am Heart Assoc*. 2020;9:e015154. doi:10.1161/jaha.119.015154
6. Lexis CP, van der Horst-Schrivers AN, Lipsic E, et al. The effect of metformin on cardiovascular risk profile in patients without diabetes presenting with acute myocardial infarction: data from the Glycometabolic intervention as adjunct to primary coronary intervention in ST elevation myocardial infarction (GIPS-III) trial. *BMJ Open Diabetes Res Care*. 2015;3:e000090. doi:10.1136/bmjdc-2015-000090
7. Jama HA, Rhys-Jones D, Nakai M, et al. Prebiotic intervention with HAMSAB in untreated essential hypertensive patients assessed in a phase II randomized trial. *Nat Cardiovasc Res*. 2023;2:35-43. doi:10.1038/s44161-022-00197-4
8. Rena G, Hardie DG, Pearson ER. The mechanisms of action of metformin. *Diabetologia*. 2017;60:1577-1585. doi:10.1007/s00125-017-4342-z
9. LaMoia TE, Shulman GI. Cellular and molecular mechanisms of metformin action. *Endocr Rev*. 2021;42:77-96. doi:10.1210/edrv/bnaa023
10. Foretz M, Guigas B, Viollet B. Metformin: update on mechanisms of action and repurposing potential. *Nat Rev Endocrinol*. 2023;19:460-476. doi:10.1038/s41574-023-00833-4
11. Bonora E, Cigolini M, Bosello O, et al. Lack of effect of intravenous metformin on plasma concentrations of glucose, insulin, C-peptide, glucagon and growth hormone in non-diabetic subjects. *Curr Med Res Opin*. 1984;9:47-51. doi:10.1185/03007998409109558
12. Sum CF, Webster JM, Johnson AB, Catalano C, Cooper BG, Taylor R. The effect of intravenous metformin on glucose metabolism during hyperglycaemia in type 2 diabetes. *Diabet Med*. 1992;9:61-65. doi:10.1111/j.1464-5491.1992.tb01716.x
13. Wu H, Esteve E, Tremaroli V, et al. Metformin alters the gut microbiome of individuals with treatment-naïve type 2 diabetes, contributing to the therapeutic effects of the drug. *Nat Med*. 2017;23:850-858. doi:10.1038/nm.4345
14. Forslund K, Hildebrand F, Nielsen T, et al. Disentangling type 2 diabetes and metformin treatment signatures in the human gut microbiota. *Nature*. 2015;528:262-266. doi:10.1038/nature15766
15. Maier L, Pruteanu M, Kuhn M, et al. Extensive impact of non-antibiotic drugs on human gut bacteria. *Nature*. 2018;555:623-628. doi:10.1038/nature25979
16. Mueller NT, Differding MK, Zhang M, et al. Metformin affects gut microbiome composition and function and circulating short-chain fatty acids: a randomized trial. *Diabetes Care*. 2021;44:1462-1471. doi:10.2337/dc20-2257
17. Pluznick JL, Protzko RJ, Gevorgyan H, et al. Olfactory receptor responding to gut microbiota-derived signals plays a role in renin secretion and blood pressure regulation. *Proc Natl Acad Sci*. 2013;110:4410-4415. doi:10.1073/pnas.1215927110
18. Bartolomaeus H, Avery EG, Bartolomaeus TUP, et al. Blood pressure changes correlate with short-chain fatty acid production potential shifts under a synbiotic intervention. *Cardiovasc Res*. 2020;116:1252-1253. doi:10.1093/cvr/cvaa083
19. Bartolomaeus H, Balogh A, Yakoub M, et al. Short-chain fatty acid propionate protects from hypertensive cardiovascular damage. *Circulation*. 2019;139:1407-1421. doi:10.1161/circulationaha.118.036652
20. Kaye DM, Shihata WA, Jama HA, et al. Deficiency of prebiotic fiber and insufficient signaling through gut metabolite-sensing receptors leads to cardiovascular disease. *Circulation*. 2020;141:1393-1403. doi:10.1161/CIRCULATIONAHA.119.043081
21. Li YJ, Chen X, Kwan TK, et al. Dietary fiber protects against diabetic nephropathy through short-chain fatty acid-mediated

- activation of G protein-coupled receptors GPR43 and GPR109A. *J Am Soc Nephrol*. 2020;31:1267-1281. doi:[10.1681/ASN.2019101029](https://doi.org/10.1681/ASN.2019101029)
22. Duscha A, Gisevius B, Hirschberg S, et al. Propionic acid shapes the multiple sclerosis disease course by an immunomodulatory mechanism. *Cell*. 2020;180:1067-1080.e1016. doi:[10.1016/j.cell.2020.02.035](https://doi.org/10.1016/j.cell.2020.02.035)
 23. Calderon-Perez L, Gosalbes MJ, Yuste S, et al. Gut metagenomic and short chain fatty acids signature in hypertension: a cross-sectional study. *Sci Rep*. 2020;10:6436. doi:[10.1038/s41598-020-63475-w](https://doi.org/10.1038/s41598-020-63475-w)
 24. Jama HA, Snelson M, Schutte AE, Muir J, Marques FZ. Recommendations for the use of dietary fiber to improve blood pressure control. *Hypertension*. 2024;81:1450-1459. doi:[10.1161/HYPERTENSIONAHA.123.22575](https://doi.org/10.1161/HYPERTENSIONAHA.123.22575)
 25. Luft FC, Mervaala E, Müller DN, et al. Hypertension-induced end-organ damage: a new transgenic approach to an old problem. *Hypertension*. 1999;33:212-218. doi:[10.1161/01.hyp.33.1.212](https://doi.org/10.1161/01.hyp.33.1.212)
 26. Bohlender J, Fukamizu A, Lippoldt A, et al. High human renin hypertension in transgenic rats. *Hypertension*. 1997;29:428-434. doi:[10.1161/01.HYP.29.1.428](https://doi.org/10.1161/01.HYP.29.1.428)
 27. Muller DN, Shagdarsuren E, Park JK, et al. Immunosuppressive treatment protects against angiotensin II-induced renal damage. *Am J Pathol*. 2002;161:1679-1693. doi:[10.1016/s0002-9440\(10\)64445-8](https://doi.org/10.1016/s0002-9440(10)64445-8)
 28. Theuer J, Dechend R, Muller DN, et al. Angiotensin II induced inflammation in the kidney and in the heart of double transgenic rats. *BMC Cardiovasc Disord*. 2002;2:3. doi:[10.1186/1471-2261-2-3](https://doi.org/10.1186/1471-2261-2-3)
 29. Shagdarsuren E, Wellner M, Braesen JH, et al. Complement activation in angiotensin II-induced organ damage. *Circ Res*. 2005;97:716-724. doi:[10.1161/01.Res.0000182677.89816.38](https://doi.org/10.1161/01.Res.0000182677.89816.38)
 30. Wellner M, Dechend R, Park JK, et al. Cardiac gene expression profile in rats with terminal heart failure and cachexia. *Physiol Genomics*. 2005;20:256-267. doi:[10.1152/physiolgenomics.00165.2004](https://doi.org/10.1152/physiolgenomics.00165.2004)
 31. Wilck N, Markó L, Balogh A, et al. Nitric oxide-sensitive guanylyl cyclase stimulation improves experimental heart failure with preserved ejection fraction. *JCI Insight*. 2018;3:e96006. doi:[10.1172/jci.insight.96006](https://doi.org/10.1172/jci.insight.96006)
 32. Fiebeler A, Schmidt F, Muller DN, et al. Mineralocorticoid receptor affects AP-1 and nuclear factor-kappaB activation in angiotensin II-induced cardiac injury. *Hypertension*. 2001;37:787-793. doi:[10.1161/01.hyp.37.2.787](https://doi.org/10.1161/01.hyp.37.2.787)
 33. Muller DN, Mullally A, Dechend R, et al. Endothelin-converting enzyme inhibition ameliorates angiotensin II-induced cardiac damage. *Hypertension*. 2002;40:840-846. doi:[10.1161/01.hyp.0000039748.88581.a0](https://doi.org/10.1161/01.hyp.0000039748.88581.a0)
 34. Katakam PV, Ujhelyi MR, Hoenig M, Miller AW. Metformin improves vascular function in insulin-resistant rats. *Hypertension*. 2000;35:108-112. doi:[10.1161/01.hyp.35.1.108](https://doi.org/10.1161/01.hyp.35.1.108)
 35. Lalau JD, Lemaire-Hurtel AS, Lacroix C. Establishment of a database of metformin plasma concentrations and erythrocyte levels in normal and emergency situations. *Clin Drug Investig*. 2011;31:435-438. doi:[10.2165/11588310-000000000-00000](https://doi.org/10.2165/11588310-000000000-00000)
 36. Hagdorn QAJ, Bossers GPL, Koop AC, et al. A novel method optimizing the normalization of cardiac parameters in small animal models: the importance of dimensional indexing. *Am J Physiol Heart Circ Physiol*. 2019;316:H1552-H1557. doi:[10.1152/ajpheart.00182.2019](https://doi.org/10.1152/ajpheart.00182.2019)
 37. Barnett-Vanes A, Sharrock A, Birrell MA, Rankin S. A single 9-colour flow cytometric method to characterise major leukocyte populations in the rat: validation in a model of LPS-induced pulmonary inflammation. *PLoS One*. 2016;11:e0142520. doi:[10.1371/journal.pone.0142520](https://doi.org/10.1371/journal.pone.0142520)
 38. Madhur Meena S, Lob Heinrich E, McCann Louise A, et al. Interleukin 17 promotes angiotensin II-induced hypertension and vascular dysfunction. *Hypertension*. 2010;55:500-507. doi:[10.1161/HYPERTENSIONAHA.109.145094](https://doi.org/10.1161/HYPERTENSIONAHA.109.145094)
 39. Sena CM, Matafome P, Louro T, Nunes E, Fernandes R, Seica RM. Metformin restores endothelial function in aorta of diabetic rats. *Br J Pharmacol*. 2011;163:424-437. doi:[10.1111/j.1476-5381.2011.01230.x](https://doi.org/10.1111/j.1476-5381.2011.01230.x)
 40. Nafisa A, Gray SG, Cao Y, et al. Endothelial function and dysfunction: impact of metformin. *Pharmacol Ther*. 2018;192:150-162. doi:[10.1016/j.pharmthera.2018.07.007](https://doi.org/10.1016/j.pharmthera.2018.07.007)
 41. Natarajan N, Hori D, Flavahan S, et al. Microbial short chain fatty acid metabolites lower blood pressure via endothelial G protein-coupled receptor 41. *Physiol Genomics*. 2016;48:826-834. doi:[10.1152/physiolgenomics.00089.2016](https://doi.org/10.1152/physiolgenomics.00089.2016)
 42. Shubitowski TB, Poll BG, Natarajan N, Pluznick JL. Short-chain fatty acid delivery: assessing exogenous administration of the microbiome metabolite acetate in mice. *Physiol Rep*. 2019;7:e14005. doi:[10.14814/phy2.14005](https://doi.org/10.14814/phy2.14005)
 43. Poll BG, Xu J, Jun S, et al. Acetate, a short-chain fatty acid, acutely lowers heart rate and cardiac contractility along with blood pressure. *J Pharmacol Exp Ther*. 2021;377:39-50. doi:[10.1124/jpet.120.000187](https://doi.org/10.1124/jpet.120.000187)
 44. Wang Y, An H, Liu T, et al. Metformin improves mitochondrial respiratory activity through activation of AMPK. *Cell Rep*. 2019;29(6):1511-1523.e5. doi:[10.1016/j.celrep.2019.09.070](https://doi.org/10.1016/j.celrep.2019.09.070)
 45. Bachem A, Makhlof C, Binger KJ, et al. Microbiota-derived short-chain fatty acids promote the memory potential of antigen-activated CD8(+) T cells. *Immunity*. 2019;51:285-297. e5. doi:[10.1016/j.immuni.2019.06.002](https://doi.org/10.1016/j.immuni.2019.06.002)
 46. Goncalves GK, Caldeira de Oliveira TH, de Oliveira BN. Cardiac hypertrophy and brain natriuretic peptide levels in an ovariectomized rat model fed a high-fat diet. *Med Sci Monit Basic Res*. 2017;23:380-391. doi:[10.12659/msmbr.907162](https://doi.org/10.12659/msmbr.907162)
 47. Almeida S, Azevedo A, Castro A, et al. B-type natriuretic peptide is related to left ventricular mass in hypertensive patients but not in athletes. *Cardiology*. 2002;98:113-115. doi:[10.1159/000066319](https://doi.org/10.1159/000066319)
 48. Burkett DA, Patel SS, Mertens L, Friedberg MK, Ivy DD. Relationship between left ventricular geometry and invasive hemodynamics in pediatric pulmonary hypertension. *Circ Cardiovasc Imaging*. 2020;13:e009825. doi:[10.1161/circimaging.119.009825](https://doi.org/10.1161/circimaging.119.009825)
 49. Travers JG, Wennersten SA, Pena B, et al. HDAC inhibition reverses preexisting diastolic dysfunction and blocks covert extracellular matrix remodeling. *Circulation*. 2021;143:1874-1890. doi:[10.1161/CIRCULATIONAHA.120.046462](https://doi.org/10.1161/CIRCULATIONAHA.120.046462)
 50. Kamo T, Akazawa H, Komuro I. Cardiac nonmyocytes in the hub of cardiac hypertrophy. *Circ Res*. 2015;117:89-98. doi:[10.1161/CIRCRESAHA.117.305349](https://doi.org/10.1161/CIRCRESAHA.117.305349)
 51. Xu L, Brink M. mTOR, cardiomyocytes and inflammation in cardiac hypertrophy. *Biochim Biophys Acta*. 2016;1863:1894-1903. doi:[10.1016/j.bbamcr.2016.01.003](https://doi.org/10.1016/j.bbamcr.2016.01.003)
 52. Oldfield CJ, Duhamel TA, Dhalla NS. Mechanisms for the transition from physiological to pathological cardiac hypertrophy. *Can J Physiol Pharmacol*. 2020;98:74-84. doi:[10.1139/cjpp-2019-0566](https://doi.org/10.1139/cjpp-2019-0566)

53. Carrillo-Salinas FJ, Ngwenyama N, Anastasiou M, Kaur K, Alcaide P. Heart inflammation: immune cell roles and roads to the heart. *Am J Pathol*. 2019;189:1482-1494. doi:[10.1016/j.ajpath.2019.04.009](https://doi.org/10.1016/j.ajpath.2019.04.009)
54. Siegismund CS, Escher F, Lassner D, et al. Intramyocardial inflammation predicts adverse outcome in patients with cardiac AL amyloidosis. *Eur J Heart Fail*. 2018;20:751-757. doi:[10.1002/ejhf.1039](https://doi.org/10.1002/ejhf.1039)
55. Usher MG, Duan SZ, Ivaschenko CY, et al. Myeloid mineralocorticoid receptor controls macrophage polarization and cardiovascular hypertrophy and remodeling in mice. *J Clin Invest*. 2010;120:3350-3364. doi:[10.1172/JCI41080](https://doi.org/10.1172/JCI41080)
56. Wenstedt EFE, van Croonenburg TJ, van den Born BH, Van den Bossche J, Hooijmans CR, Vogt L. The effect of macrophage-targeted interventions on blood pressure - a systematic review and meta-analysis of preclinical studies. *Transl Res*. 2021;230:123-138. doi:[10.1016/j.trsl.2020.11.002](https://doi.org/10.1016/j.trsl.2020.11.002)
57. Harwani SC. Macrophages under pressure: the role of macrophage polarization in hypertension. *Transl Res*. 2018;191:45-63. doi:[10.1016/j.trsl.2017.10.011](https://doi.org/10.1016/j.trsl.2017.10.011)
58. Chang PV, Hao L, Offermanns S, Medzhitov R. The microbial metabolite butyrate regulates intestinal macrophage function via histone deacetylase inhibition. *Proc Natl Acad Sci USA*. 2014;111:2247-2252. doi:[10.1073/pnas.1322269111](https://doi.org/10.1073/pnas.1322269111)
59. Schulthess J, Pandey S, Capitani M, et al. The short chain fatty acid butyrate imprints an antimicrobial program in macrophages. *Immunity*. 2019;50:432-445.e7. doi:[10.1016/j.immuni.2018.12.018](https://doi.org/10.1016/j.immuni.2018.12.018)
60. Asarat M, Apostolopoulos V, Vasiljevic T, Donkor O. Short-chain fatty acids regulate cytokines and Th17/Treg cells in human peripheral blood mononuclear cells in vitro. *Immunol Investig*. 2016;45:205-222. doi:[10.3109/08820139.2015.1122613](https://doi.org/10.3109/08820139.2015.1122613)
61. Du HX, Yue SY, Niu D, Liu C, et al. Gut microflora modulates Th17/Treg cell differentiation in experimental autoimmune prostatitis via the short-chain fatty acid propionate. *Front Immunol*. 2022;13:915218. doi:[10.3389/fimmu.2022.915218](https://doi.org/10.3389/fimmu.2022.915218)
62. Ramirez FD, Motazedian P, Jung RG, et al. Sex bias is increasingly prevalent in preclinical cardiovascular research: implications for translational medicine and health equity for women: a systematic assessment of leading cardiovascular journals over a 10-year period. *Circulation*. 2017;135:625-626. doi:[10.1161/CIRCULATIONAHA.116.026668](https://doi.org/10.1161/CIRCULATIONAHA.116.026668)
63. Bauer Y, Hess P, Qiu C, et al. Identification of cathepsin L as a potential sex-specific biomarker for renal damage. *Hypertension*. 2011;57:795-801. doi:[10.1161/hypertensionaha.110.157206](https://doi.org/10.1161/hypertensionaha.110.157206)

SUPPORTING INFORMATION

Additional supporting information can be found online in the Supporting Information section at the end of this article.

How to cite this article: Wimmer MI, Bartolomaeus H, Anandakumar H, et al. Metformin modulates microbiota and improves blood pressure and cardiac remodeling in a rat model of hypertension. *Acta Physiol*. 2024;240:e14226. doi:[10.1111/apha.14226](https://doi.org/10.1111/apha.14226)